

Epitaxial Nature of $\text{CH}_3\text{NH}_3\text{PbI}_3$ Thin Films Grown on $\text{CH}_3\text{NH}_3\text{PbCl}_3$ Single Crystal Substrates

Zihao Liu, Tomonori Matsushita and Takashi Kondo

The University of Tokyo

4-6-1, Komaba, Meguro-ku, Tokyo 153-8904, Japan

Phone: +81-3-5452-5170 E-mail: liuzihao@castle.t.u-tokyo.ac.jp

Abstract

We have successfully fabricated all-perovskite heterostructure by epitaxial growth of $\text{CH}_3\text{NH}_3\text{PbI}_3$ on $\text{CH}_3\text{NH}_3\text{PbCl}_3$ single crystal substrates. Inter-diffusion of halogen ions, which we suffered from on bromide substrates, was partially suppressed by using combination of Cl/I ions owing to larger difference in ion radii.

1. Introduction

Metal halide perovskites have attracted significant attention owing to the promising scenario of being the next generation photovoltaic materials since the emergence in 2009 [1]. The materials exhibit unique properties such as strong absorption, long carrier lifetime and long diffusion length. Recently the power conversion efficiencies of perovskite solar cells have reached 25.2% [2]. So far most of these devices have been based on polycrystalline thin films grown by spin coating. To further study the properties of perovskites, single crystals are required, and we believe that single crystalline perovskites will also play an important role in the field of functional devices.

Previously, Chen *et al.* have reported the strain engineering of an epitaxial $\text{CH}(\text{NH}_2)_2\text{PbI}_3$ thin film on $\text{CH}_3\text{NH}_3\text{Pb}(\text{BrI})_3$ alloy substrates, where the A site ion of the film is different from that of the substrates [3]. We have tried to grow $\text{CH}_3\text{NH}_3\text{PbI}_3$ on $\text{CH}_3\text{NH}_3\text{PbBr}_3$ single crystal substrates with the same A site ion, but only obtained $\text{CH}_3\text{NH}_3\text{Pb}(\text{BrI})_3$ alloy epitaxial thin films due to inter-diffusion of halogen ions [4]. In order to obtain heterostructure of pure perovskites, we replaced the substrate with $\text{CH}_3\text{NH}_3\text{PbCl}_3$, which has a larger ion radius difference than $\text{CH}_3\text{NH}_3\text{PbBr}_3$ to suppress the diffusion. Here we report the epitaxial growth of a $\text{CH}_3\text{NH}_3\text{PbI}_3$ film on a $\text{CH}_3\text{NH}_3\text{PbCl}_3$ substrate and its characterization by X-ray diffraction (XRD).

2. Experimental

$\text{CH}_3\text{NH}_3\text{PbCl}_3$ single crystal substrates were prepared by inverse temperature crystallization [5]. 1 mol/L precursor of $\text{CH}_3\text{NH}_3\text{Cl}$ and PbCl_2 dissolved in dimethyl sulfoxide and N,N-dimethylformamide (1:1 v/v) were heated to around 55°C for 6 hours. Then we obtained transparent bulk $\text{CH}_3\text{NH}_3\text{PbCl}_3$ single crystals. The sizes are $4 \times 4 \times 1 \text{ mm}^3$. The upper surface of the single crystal was determined to be (001) surface by XRD. We used the as-grown surfaces of chloride single crystals without any treatment.

Then 160-nm-thick $\text{CH}_3\text{NH}_3\text{PbI}_3$ films were deposited on

the as grown (001) surfaces of single crystal substrates by co-evaporating $\text{CH}_3\text{NH}_3\text{I}$ and PbI_2 . The supply of PbI_2 was controlled by a quartz crystal microbalance at a rate of 0.2 Å/s, while MAI was monitored by the chamber pressure and was kept at 0.0015 Pa. The temperature of the substrate was kept at 21°C throughout the evaporation by cooling water. After the evaporation, the transparent single crystal turns into a darkish brown color.

3. Characterization and Analysis

We investigated the fabricated sample by using XRD. Figure 1 shows XRD pattern ($2\theta/\omega$ scan) of the sample. The result clearly shows that the index of upper surface of the single crystal substrate is (001). Apart from the substrate (001) and (002) peaks, we observe other two peaks (the sets of (002) and (110), and of (004) and (220)) of $\text{CH}_3\text{NH}_3\text{PbI}_3$ but no peak of PbI_2 , indicating that we have successfully grown $\text{CH}_3\text{NH}_3\text{PbI}_3$ on the $\text{CH}_3\text{NH}_3\text{PbCl}_3$ single crystal substrate. To further verify the existence of pure perovskites, we also measured the photoluminescence spectrum of the sample at room temperature and observed the emission peak at the bandgap of $\text{CH}_3\text{NH}_3\text{PbI}_3$ (1.62 eV).

The inset of Fig. 1 shows a closer view of the substrate (002) peak. A shoulder peak emerged on the left side corresponding to the formation of a $\text{CH}_3\text{NH}_3\text{Pb}(\text{Cl}_{1-x}\text{I}_x)_3$ perovskite alloy layer. The small peak in the middle may be caused by the nonuniform distribution of iodine ions in the substrate. Reciprocal space map (RSM) was also used to analyze the thin film. Figures 2 shows the RSM of asymmetric reflection peak (024). Apart from the relatively intense substrate peak, we can observe a broadening downward after evaporation as

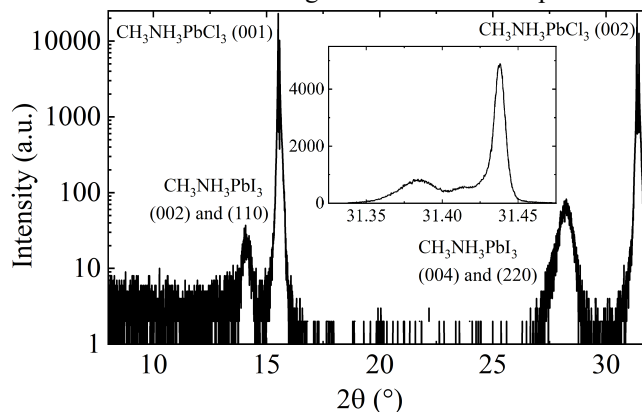


Figure 1 $2\theta/\omega$ XRD pattern of the fabricated thin film. The inset shows an expanded view of the substrate (002) peak.

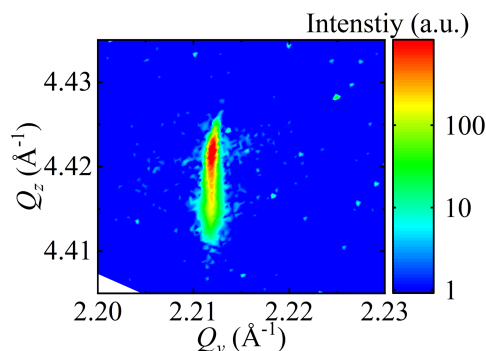


Figure 2 RSM of the sample near asymmetric reflection peak (024) of substrates.

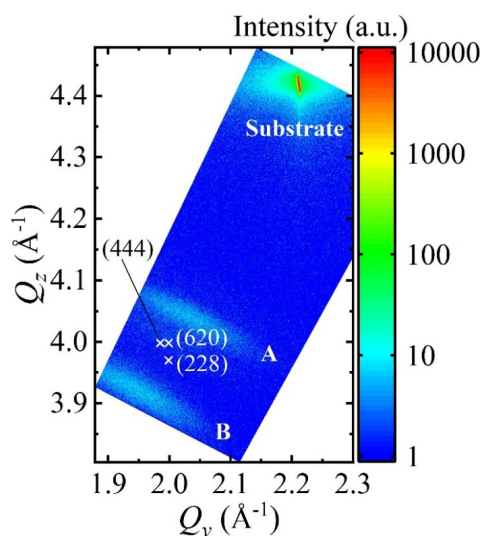


Figure 3 RSM of larger area near asymmetric reflection peak (024) of substrates. \times marks denote the calculated positions for each plane.

shown in Fig. 2. This clearly shows that the pseudomorphic (almost fully strained) perovskite alloy is also formed. According to the reported Poisson's ratio of $\text{CH}_3\text{NH}_3\text{PbCl}_3$ [6], we estimated that the unstrained lattice constant of perovskite alloy is 5.691 Å. Using the lattice constant data of $\text{CH}_3\text{NH}_3\text{PbI}_3$ [7] and assuming Vegard's law, the composition of iodine is estimated to be $x=0.8\%$, which is smaller than the bromide perovskite substrate case (3.2%) [4].

Another two peaks emerge in larger-area RSM around substrate (024) peak (Fig. 3). We presume that those two peaks (A and B) in Fig. 3 originate from epitaxial $\text{CH}_3\text{NH}_3\text{PbI}_3$ thin film, although the obtained positions of the peaks are relatively far from those calculated from $\text{CH}_3\text{NH}_3\text{PbI}_3$ lattice constants. Since those peaks exist on the line connecting the origin and substrate (024) peak, the thin film is fully relaxed. We calculated the peak positions of relaxed $\text{CH}_3\text{NH}_3\text{PbI}_3$ (228), (444) or (620), which correspond to cases where c axis of $\text{CH}_3\text{NH}_3\text{PbI}_3$ is parallel to the c , b or a axis of $\text{CH}_3\text{NH}_3\text{PbCl}_3$, respectively. (In all the cases, the $[\text{PbI}_6]^{4-}$ octahedrons are stacked in the same way as substrate.) The calculated positions of the three reflections are significantly different from those obtained in experiment. However, since the calculated positions of (620) and (444) are too close to distinguish, the two peaks obtained in the experiment are

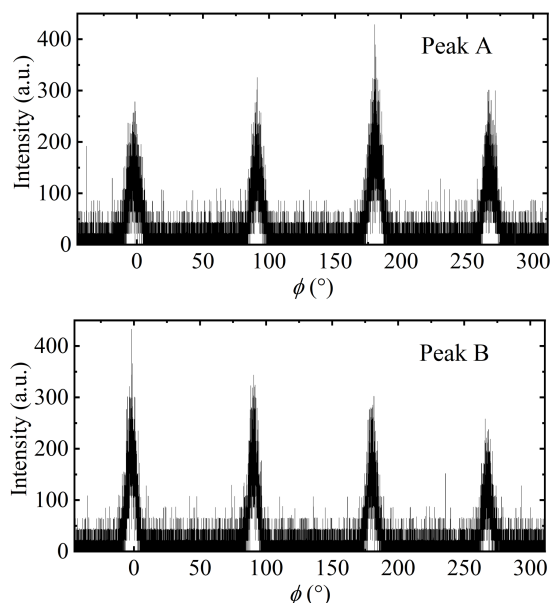


Figure 4 ϕ scan of the two peaks (A and B) in Fig.3.

consistent with the calculated three peaks (Fig. 3). To investigate the symmetry of the thin film, we measured ϕ scans of A and B peaks (Fig. 4). Four peaks for each scan were detected at $\phi = 0^\circ, 90^\circ, 180^\circ$ and 270° , indicating that the thin film was epitaxially grown. Since PbI_2 exhibits hexagonal structure (6-fold symmetry), we attribute peaks A and B to epitaxial $\text{CH}_3\text{NH}_3\text{PbI}_3$ thin film.

4. Conclusion

We have successfully grown a $\text{CH}_3\text{NH}_3\text{PbI}_3$ epitaxial thin film on the $\text{CH}_3\text{NH}_3\text{PbCl}_3$ single crystal substrate. Compared with our previous result on the $\text{CH}_3\text{NH}_3\text{PbBr}_3$ single crystal substrate, the ion interdiffusion is suppressed owing to the larger difference in ion sizes. Larger difference between bandgaps of $\text{CH}_3\text{NH}_3\text{PbI}_3$ and $\text{CH}_3\text{NH}_3\text{PbCl}_3$ is, without doubt, beneficial for fabricating quantum-well devices with strong quantum confinement effects.

Reference

- [1] A. Kojima, K. Teshima, Y. Shirai and T. Miyasaka, *J. Am. Chem. Soc.* **131** (2009) 6050.
- [2] <https://www.nrel.gov/pv/assets/pdfs/best-research-cell-efficiencies.20200406.pdf>
- [3] Y. Chen, Y. Lei, Y. Li, Y. Yu, J. Cai, M. Chiu, R. Rao, Y. Gu, C. Wang, W. Choi, H. Hu, C. Wang, Y. Li, J. Song, J. Zhang, B. Wi, M. Lin, Z. Zhang, A. E. Islam, B. Maruyama, S. Dayeh, L. Li, K. Yang, Y. Lo and S. Xu, *Nature* **577** (2020) 209.
- [4] K. Kimura, Y. Nakamura, T. Matsushita and T. Kondo, *Jpn. J. Appl. Phys.* **58** (2019) SBBF04.
- [5] G. Maculan, A. D. Sheikh, A. L. Abdelhady, M. I. Saidaminov, M. A. Haque, B. Murali, E. Alarousu, O. F. Mohammed, T. Wu and O. M. Bakr, *J. Phys. Chem. Lett.* **6** (2015) 3781.
- [6] J. Lee, Z. Deng, N. C. Bristowe, P. D. Bristowe and A. K. Cheetham, *J. Mater. Chem. C* **6** (2018) 12252.
- [7] Y. Nakamura, N. Shibayama, A. Hori, T. Matsushita, H. Segawa and T. Kondo, *Inorg. Chem.* **59** (2020) 6709.